Proceedings of the ASME 2009 International Design Engineering Technical Conferences & Computers and Information in Engineering Conference
IDETC/CIE 2009
August 30 - September 2, 2009, San Diego, California, USA

DETC2009-87488

EMPIRICAL SIMILARITY ANALYSIS USING ADAPTIVE TRIGONOMETRIC FUNCTIONS

Srikanth Tadepalli
Department of Mechanical Engineering
The University of Texas at Austin
Austin, TX 78712
512 – 762 – 0247
tsrikanth@mail.utexas.edu

Kristin L. Wood
Department of Mechanical Engineering
The University of Texas at Austin
Austin, TX 78712
512 – 471 – 0095
wood@mail.utexas.edu

ABSTRACT
Similarity methods have been widely employed in engineering design and analysis to model and scale complex systems. The Empirical Similitude Method (ESM) is one such method based on the use of experimental data. Using a variant of the similitude process involving experimental data, we present in this paper, the use of advanced numerical approximations, trigonometric functions in particular to model and predict the performance of design artifacts. Specifically, an airfoil design is modeled, and the values of the drag coefficient are estimated based on the advanced ESM. Intermediate test specimens are used to correlate experimental data to produce the required prediction parameters. Mathematical development and error analysis are also elaborated by delving into continuity and adaptivity features of numerical algorithms.

KEYWORDS
Empirical Similarity, Model, Model Specimen, Product, Product Specimen, Trigonometric Functions, Continuity, Adaptivity

INTRODUCTION
Engineers often deal with complex analytical relations arising from associating different variables affecting a mechanical system. Sometimes, identifying the influencing variables alone becomes a challenge and any incorrect choice leads to erroneous modeling laws and uncertain physical interpretations. Developing these mathematical identities is a difficult task in itself even if an engineer has successfully isolated the key parameters affecting a system. Experimentation is thus, often times the desired alternative as its successful execution produces numerical values that are both repeatable and reproducible. Numerical values provide an alternative approach compared to closed-form solutions when such solutions do not exist or are difficult to develop. Engineering testing and analysis performed with minimal human interaction, bias and error also yields accurate results. However, it is imperative that these experimental values be used judiciously to understand and model (and sometimes predict) the performance of a system [David et al., 1982].

Experimentation can also incorporate the benefit of scaling a system (using the Buckingham π method) to either account for geometric constraints or test conditions (see Figure 1), both of which cause considerable restrictions due to size limitations and necessity to *mimic* physical reality respectively. However, if both these impediments can be circumvented, then substantial quantitative benefit can be achieved using experimental data. *Models* (scaled simpler geometries) and *products* (actual systems) can thus be related [Baker et al., 1991, Langhaar, 1951] to each other using experimental response values resulting in significant time and cost savings – an avoidable expense that would have occurred had the full scale product been tested itself. Expanding this principle, we explore novel application of such empirical relations so that numerical values can be correlated rather than variables and parameters to predict a systems performance during design.

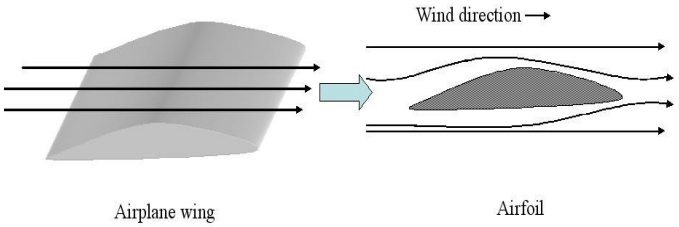

Figure 1. An airplane wing (*product*) being evaluated as a simplified airfoil (*model*) using the Buckingham π method

BACKGROUND INFORMATION
Assume that a complex system called *product* is being parametrically designed or evaluated using similarity techniques [Schnittger, 1988], a particular state or parameter (X_p) being the variable of interest. If this system is intricate implying complexity in either geometry or material properties, then testing the system would require unnecessary investment

in manufacturing a full-scale test specimen (or prototype) for experimentation. While the geometric impediment can be overcome using modern rapid prototyping processes [Dornfeld, 1995], fabricating a specimen to have all the desired material properties as that of the *product* would not be ideal due to cost constraints, especially since it is going to be used primarily for testing and is not an end product in itself. The problem compounds when the *product* is to be made of multiple materials as dictated by modern day design requirements of light weight, environmentally friendly and aesthetically pleasing structures. This requirement means that the specimen must also be made from multiple materials, which is not cost effective.

To simplify these overburdening requirements [Cho, 1998, Dutson, 2002] developed the method of Empirical Similarity (ESM) (see Figure 2) where the geometric simplification is achieved by replacing a complex *product* with a simplified *product specimen* and *model*. Thus, a simplified, easy to machine (and/or manufacture) alternative is created in the form of *product specimen* while the *model* provides the benefit of a single material structure thereby incorporating uniformity. Thus, either material or geometry (or both) can be changed by keeping the simplified representations distinct yet experimenting with variations of each. Note that the *model* in ESM is different from that defined in the Buckingham π method.

Hence, the product state vector ($\boldsymbol{X_p}$) can be represented as a function of the geometry simplified *product specimen* ($\boldsymbol{X_{ps}}$) and the material simplified *model* ($\boldsymbol{X_m}$). However the change in the geometry and material properties still needs to be quantified between the three structures. Remember that the *product* could still be in the design phase thus lacking any physical form or presence *i.e.*, could still be hypothetical. However, change in geometry (F) and the change in material conditions (S) have to be quantified without actually testing the *product*, the experimentation of which would negate the reason to develop any simplified representations *i.e.*, the *product specimen* and the *model*. But the *product specimen* and the *model* are independent entities and share no similarity with each other. Thus, a third simplification is sought called the *model specimen* ($\boldsymbol{X_{ms}}$) which couples the *product specimen* through similar geometry and the *model* through similar material. Using these three geometries, the two required transformations in form (F) and material (S) can be achieved using the following mathematical identities. Thus, $\boldsymbol{X_{ps}}$, $\boldsymbol{X_m}$ and $\boldsymbol{X_{ms}}$ being the set of measured data points indicating functional values (like temperature) in the *product specimen*, *model* and *model specimen* respectively, we have,

$$S = f(X_{ps}, X_{ms}) \tag{1}$$

$$F = g(X_m, X_{ms}) \tag{2}$$

and

$$\begin{aligned} X_p &= SX_m = f(X_{ps}, X_{ms})X_m \\ &= FX_{ps} = g(X_m, X_{ms})X_{ps} \end{aligned} \tag{3}$$

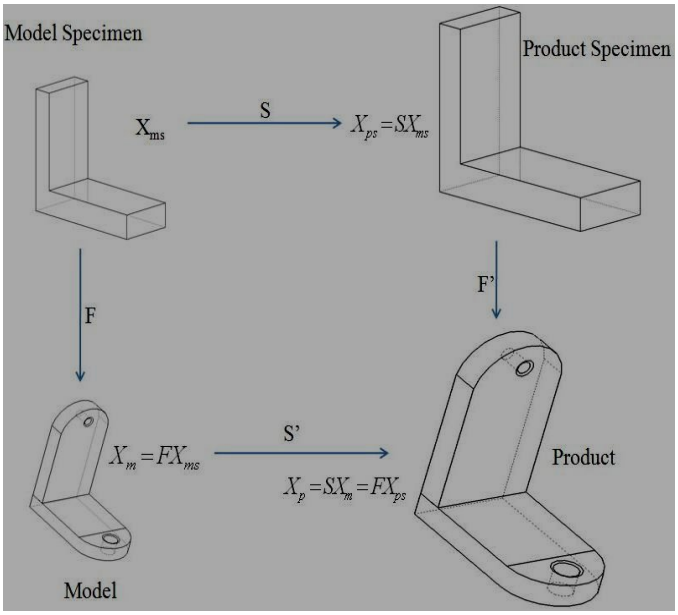

Figure 2. Empirical Similitude Method

The response of the *product* can thus be approximated using the correlation between the *model*, *product specimen* and *model specimen*. Notice from Figure 2 that the *product specimen* is a simplified form of the *product* without any curves or holes and is identical to the *model specimen* in shape. The *model* is identical to the *product* in shape but is a simplification in material form[1]. Thus, shape is consistent horizontally and material remains the same vertically. Rewriting equations 1 – 3, the ESM problem can be formally identified using,

$$X_{ps} = f_1(X_{ms}) \tag{4}$$

$$X_m = g_1(X_{ms}) \tag{5}$$

$$X_p = f_1(X_m) = g_1(X_{ps}) = (f_1 * g_1)X_{ms} \tag{6}$$

$$X_p = h_1(X_{ms}, X_{ps}, X_m) \tag{7}$$

where f_1 and g_1 are functional forms carry information regarding material translation (S) and form transformation (F) respectively. Notice that functions are convoluted when relating *product* and *model specimen* as simple multiplication

[1] Manufacturing the *model* is not an issue as it is intended to be made from Rapid Prototyping (RP) processes using polymer materials. The *product* however cannot be directly fabricated using RP because it sometimes needs to made from metal that can only be machined.

does not convey information regarding material and geometry changes. Convolution provides necessary integration and interaction of material properties *as* geometry modifies.

Further, since the process is symmetric and the transformations *S* and *F* are assumed to be independent, the translation from *model* to *product* (*S'*) and *product specimen* to product (*F'*) must also be independent. Hence, *S'* is synonymous with *S* and *F'* is identical to *F*. Also note that while the description provided thus far is a general usage of the ESM procedure capturing geometric and material changes, the analysis and independent transformations can include other variations like differences in test conditions, boundary conditions, input parameters etc.

TEST FOR NON-LINEARITY

Having established the mathematical formulation of ESM, we now consider the possibility of the functions *f* and *g* being non-linear. The set $\{(X_{ms}), (X_{ps})$ and $(X_m)\}$ indicating experimentally measured numerical values can be analyzed to identify non-linearity. This is achieved through the Pearson's product-moment correlation coefficient [Spiegel, 1992] given by,

$$r = \frac{\left\langle \sum XY - \frac{\sum X \sum Y}{N} \right\rangle}{\sqrt{\left\langle \sum X^2 - \frac{\left(\sum X\right)^2}{N} \right\rangle \left\langle \sum Y^2 - \frac{\left(\sum Y\right)^2}{N} \right\rangle}} \qquad (8)$$

Note that the Pearson's test assumes linearity between the two variables *X* and *Y* and a correlation value of 1 or -1 indicates perfect positive or negative linearity and 0 represents no linear relation between the two variables. Values are very rarely 1, -1 or 0 but closer the value of the coefficient to the value of 0[2] greater the accuracy of the non-linearity assumption. Hence r^2 indicates the degree of variation in the estimation which can be interpreted as the measure of variability caused in the variable *Y* due to the variation in *X*. Therefore, the test performed on the set $\{(X_{ms}), (X_{ps})$ and $(X_m)\}$ allows to determine the effects of non-linearity between each state vector unequivocally. This test is simple and for a limited number of observations like in ESM, it is quite practical for motivating use of non-linear methods of which trigonometric functions are one. The reason trigonometric functions are chosen is because they have enough degrees of freedom to offer the flexibility of combining piece-wise continuous and adaptive solutions at intermediate junction points such that first order continuity can be achieved in the global solution as is shown next.

[2] Note also that a value much lesser than 1 only signifies non-existence of a linear relationship but does not discount the possible existence of a non-linear relationship.

CONTINUITY AND ADAPTIVITY

The response of mechanical systems to inputs is always smooth and continuous, and indicates a faulty working system otherwise. Further, the response can also be highly non-linear due to friction, heat and other losses. This non-linearity is palpable in fluid systems where viscosity and turbulence is noticed quite often [Binder, 1973].

When such non-linearities are modeled mathematically, it is prudent to discretize the working domain[3] into several sub-domains or intervals so that each interval can be studied closely and appropriate curves can be fitted. Thus, a customized analytical relation can be achieved for each interval complete with minimal error and desired continuity. Depending on the degree of non-linearity[4], it is wise to use piece-wise continuous functions[5] that model individual intervals rather than use one global polynomial [Kendall, 1988]. Using local adaptive functions also allows determination of the right order in each interval so that the local error is minimized. Hence adaptivity allows close mathematical approximations of highly non-linear curves. However, the downside of discretization is the necessity to combine solutions at junction points by merging the interval specific solutions seamlessly *i.e.*, maintaining position and slope continuity at the junction points, which is mandated due to the smooth nature of the response curve. This is achieved by forcing the condition that the numerical values of the function and the first derivative evaluated at the junction points be identical for both participating intervals. The necessity to maintain such rigid conditions is illustrated below (see Figure 3) where the effect of forcing higher order continuity as against simple position correction clearly introduces smoothness in the curve[6].

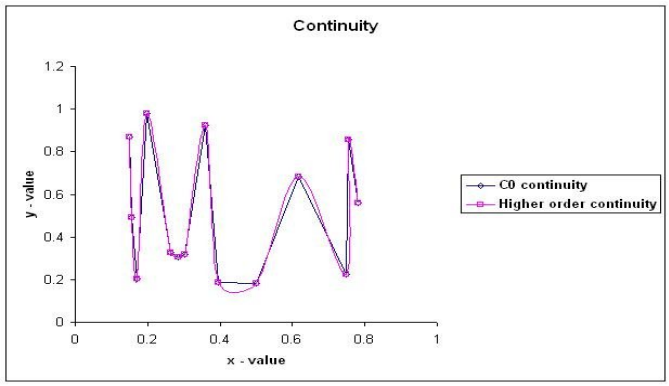

Figure 3. Effect of higher order continuity

[3] The number of data points in the working range.
[4] As suggested by Pearson's test.
[5] Trigonometric functions in this paper.
[6] Note that the graph is only an illustration comparing linear functions and higher order polynomials to convey the idea of relative smoothness and continuity, and does not incorporate trigonometric functions.

Thus, a marching solution is setup as the entire data set is traversed where each individual interval is mapped with a custom trigonometric function, discussed in the next section, that minimizes error in that interval. Enforcing slope and position continuity conditions allows development of a global solution which is smooth. This strategy models individual interval peaks and troughs which would have been impossible had a single global polynomial been used.

TRIGONOMETRIC APPROXIMATIONS

Trigonometric functions are derived from the classic Fourier series analysis [Linz, 1979] where sinusoidal curves are described to mathematically define the behavior of a periodic function. The standard model of a Fourier series is given by,

$$f(x) = a_1 + \sum_{n=1}^{r} b_n \cos nx + \sum_{n=1}^{r} c_n \sin nx \qquad (9)$$

where the coefficients of the series capture the degree of scaling. Hence, a set of discrete data points can be modeled using a smooth periodic curve like the Fourier series. Such a formulation allows fitting interval specific sinusoidal functions so that close approximations can be obtained. Further, since a functional form exists, error analysis can be performed by comparing the actual value and the fitted value. The potential complication that might arise due to Gibbs phenomenon is not applicable here as there are no jump continuities in the working domain to negotiate and the solution curve is assumed to be smooth as alluded to earlier. We modify the Fourier series technique to adapt to ESM as is shown next.

MATHEMATICAL FORMULATION FOR ESM

The effect of trigonometric smoothing is realized in ESM by [Linz, 1979],

$$x_p = a_1 + \sum_{n=1}^{r} b_n \cos nx_m + \sum_{n=1}^{r} c_n \sin nx_m \qquad (10)$$

where constants a_1, b_n and c_n are derived using,

$$x_{ps} = a_1 + \sum_{n=1}^{r} b_n \cos nx_{ms} + \sum_{n=1}^{r} c_n \sin nx_{ms} \qquad (11)$$

Similarly,

$$x_m = a_1^* + \sum_{n=1}^{r} b_n^* \cos nx_{ms} + \sum_{n=1}^{r} c_n^* \sin nx_{ms} \qquad (12)$$

In each interval, a trigonometric function is constructed starting from order n = 1, requiring 2 states of $\{x_{ms,i}, x_{ps,i}\}$ and slope at one of the end points to establish scale trigonometric and, 2 states of $\{x_{ms,i}, x_{m,i}\}$ and slope at one of the end points to establish form trigonometric such that,

$$\begin{pmatrix} x_{ps,1} \\ x_{ps,3} \\ x'_{ps,3} \end{pmatrix}^{est} = \begin{pmatrix} 1 & \cos x_{ms,1} & \sin x_{ms,1} \\ 1 & \cos x_{ms,3} & \sin x_{ms,3} \\ 0 & -\sin x_{ms,3} & \cos x_{ms,3} \end{pmatrix} \begin{pmatrix} a_1 \\ b_1 \\ c_1 \end{pmatrix}$$

and

$$\begin{pmatrix} x_{m,1} \\ x_{m,3} \\ x'_{m,3} \end{pmatrix}^{est} = \begin{pmatrix} 1 & \cos x_{ms,1} & \sin x_{ms,1} \\ 1 & \cos x_{ms,3} & \sin x_{ms,3} \\ 0 & -\sin x_{ms,3} & \cos x_{ms,3} \end{pmatrix} \begin{pmatrix} a_1^* \\ b_1^* \\ c_1^* \end{pmatrix}$$

such that for intermediate point 2,

$$\in_2^{n=1} = \left\| x_{ps,2}^{est} - x_{ps,2} \right\|_{L^2} \qquad (13)$$

and

$$\varepsilon_2^{n=1} = \left\| x_{m,2}^{est} - x_{m,2} \right\|_{L^2} \qquad (14)$$

where $\in_2$ and ε_2 are errors measured in the L^2 norm[7] between the estimated value (*est*) and the actual value. The curve fitting process employs higher order approximations iteratively till current net error is numerically higher in magnitude than previous error. In general, for every interval *k*,

$$\begin{pmatrix} x_{ps,1} \\ \vdots \\ x_{ps,n} \\ x'_{ps,n} \end{pmatrix}^{est} = \begin{pmatrix} 1 & \cos & \sin \\ \vdots & \vdots & \vdots \\ 1 & \cos & \sin \\ 0 & -\sin & \cos \end{pmatrix}_{2n+1} \begin{pmatrix} a \\ b \\ c \end{pmatrix}_{2n+1}$$

and

$$\begin{pmatrix} x_{m,1} \\ \vdots \\ x_{m,n} \\ x'_{m,n} \end{pmatrix}^{est} = \begin{pmatrix} 1 & \cos & \sin \\ \vdots & \vdots & \vdots \\ 1 & \cos & \sin \\ 0 & -\sin & \cos \end{pmatrix}_{2n+1} \begin{pmatrix} a^* \\ b^* \\ c^* \end{pmatrix}_{2n+1}$$

such that for any intermediate point *t* in interval *k*,

$$\in_{\min} = \min \left\| x_{ps,t}^{est} - x_{ps,t} \right\|_{L^2} \qquad (15)$$

and

[7] The L^2 norm is used because errors can be negative but this norm forces square of the numerical value which is always positive regardless of the individual error value and thus easier to deal with.

$$\varepsilon_{\min} = \min \left\| x_{m,t}^{est} - x_{m,t} \right\|_{L^2} \tag{16}$$

The technique iterates till $\in_{\min}$ and $\varepsilon_{\min}$ are established for an optimal order *n* (depending on availability of data) in each interval such that net system root mean square error,

$$\varepsilon_{sys}^{n} = \left(\in_{RMS} \ \varepsilon_{RMS} \right) \leq \varepsilon_g$$

where ε_g is allowable global tolerance and for *n* intervals,

$$\in_{RMS} = \sqrt{\frac{\sum_{k=1}^{n} \left(\in_{\min,k} \right)^2}{n}} \tag{17}$$

$$\varepsilon_{RMS} = \sqrt{\frac{\sum_{k=1}^{n} \left(\varepsilon_{\min,k} \right)^2}{n}} \tag{18}$$

The RMS error is chosen since it represents the global average of all minimum errors in individual intervals. Higher order continuity is ensured at all junction points *i* such that,

$$\begin{aligned} &- b_n \sin n x_{ms,i^-} + c_n \cos x_{ms,i^-} = \\ &- b_n \sin n x_{ms,i^+} + c_n \cos x_{ms,i^+} \end{aligned} \tag{19}$$

Consider a numerical example for better understanding of the mathematical development. Assume that the *model specimen* and the *product specimen* have hypothetical values given by,

$$x_{ms} = \begin{pmatrix} 325 \\ 368 \\ 417 \\ 484 \\ 543 \end{pmatrix}, \quad x_{ps} = \begin{pmatrix} 416 \\ 488 \\ 525 \\ 573 \\ 635 \end{pmatrix}$$

we have,

$$\begin{aligned} 416 &= \left(\frac{180}{\pi}\right)\left[a_1 + b_1 \cos\left(\frac{325\pi}{180}\right) + c_1 \sin\left(\frac{325\pi}{180}\right)\right] \\ 525 &= \left(\frac{180}{\pi}\right)\left[a_1 + b_1 \cos\left(\frac{417\pi}{180}\right) + c_1 \sin\left(\frac{417\pi}{180}\right)\right] \\ 525 &= \left(\frac{180}{\pi}\right)\left[a_2 + b_2 \cos\left(\frac{417\pi}{180}\right) + c_2 \sin\left(\frac{417\pi}{180}\right)\right] \\ 635 &= \left(\frac{180}{\pi}\right)\left[a_2 + b_2 \cos\left(\frac{543\pi}{180}\right) + c_2 \sin\left(\frac{543\pi}{180}\right)\right] \end{aligned}$$

Slope at the intersecting point (417, 525) is matched for both the intervals and slope at the right extreme of the second interval is assumed to be zero such that,

$$\begin{aligned} &- b_1 \sin\left(\frac{417\pi}{180}\right) + c_1 \cos\left(\frac{417\pi}{180}\right) = \\ &- b_2 \sin\left(\frac{417\pi}{180}\right) + c_2 \cos\left(\frac{417\pi}{180}\right) \\ &- b_2 \sin\left(\frac{543\pi}{180}\right) + c_2 \cos\left(\frac{543\pi}{180}\right) = 0 \end{aligned}$$

thus solving for 6 unknowns using 6 equations. The values of the constants are evaluated to be,

$$\begin{pmatrix} a_1 \\ b_1 \\ c_1 \\ a_2 \\ b_2 \\ c_2 \end{pmatrix} = \begin{pmatrix} 8.26938 \\ -0.333714 \\ 1.28221 \\ 9.8737 \\ -1.20749 \\ -0.0632817 \end{pmatrix}$$

hence creating the functions,

$$\begin{aligned} x_{ps,h=1} &= 8.26938 - 0.333714 \cos x_{ms} + 1.28221 \sin x_{ms} \\ x_{ps,h=2} &= 9.8737 - 1.20749 \cos x_{ms} - 0.0632817 \sin x_{ms} \end{aligned}$$

Predicting and estimating errors at the discarded points (368, 488) and (484, 573) using the two functions respectively we have,

$$\begin{aligned} x_{ps.est}(368,488) &= 465.091 \\ x_{ps.est}(484,573) &= 601.402 \\ \in_1 &= 22.909 \\ \in_2 &= 28.402 \end{aligned}$$

and

$$S = \begin{pmatrix} 8.26938 & -0.333714 & 1.28221 \\ 9.8737 & -1.20749 & -0.0632817 \end{pmatrix}$$

Bear in mind that these functions are for illustration alone and are first order in both intervals. The algorithm however searches for the optimal order in each interval before diminishing returns is observed. The form transformation is developed using a similar procedure. The only limitation of the adaptive trigonometric method is a potential complication when extremely small values are encountered which tend to be approximated or extremely large values are observed which

cause quadrant specific multi-valued behavior in sinusoidal functions. Also, in adaptive methods, individual interval solutions need to be "summed" for a global response curve. The biggest and single most important innovation in development of this process is that use of true adaptivity where interval length and function order are customized. A practical application of this technique is shown next with a minor variation in the problem statement after the algorithm and procedure are summarized below (see Figure 4).

Algorithm for construction of adaptive trigonometric functions

Step 1: Set $\varepsilon_g \rightarrow tol$. Go to step 2.

Initial value of acceptable global error to be equal to some fixed finite tolerance.

Step 2: Set $m \rightarrow 1$, Set $n \rightarrow m$, Set $h \rightarrow 1$. Go to step 3.

Initial search index of function, *n*, set to degree 1. This implies that a first order trigonometric function is fitted in each interval. Further, we have 3 DOF and hence each interval has 3 nodes - 2 to approximate the function with slope information and 1 to interpolate and verify. This is also the first interval.

Step 3: Set $z_i \rightarrow \{x_{ms,i}, x_{ps,i}\}$, the end points of each interval. Go to step 4.

If the material is isotropic throughout, then each interval is of uniform length else interval length is determined by end points located exactly where a change in material property occurs.

Step 4: Fit $x_{ps}^{est} = a_1 + b_1 \cos x_{ms} + c_1 \sin x_{ms}$. Go to step 5.

Curve that fits distribution of values at points between the two geometries in the particular interval.

Step 5: Estimate local error $\in_{l,i} \rightarrow \left\| x_{ps}^{est} - x_{ps} \right\|_{L^2}$ at each intermediate point. Go to step 6.

L^2 norm is chosen as it accounts for possible negative values in estimating local errors.

Step 6: Estimate minimum of local errors $\in_{\min} \rightarrow \min\{\in_{l.i}\}$. Go to step 7.

Step 7: Include next data point, modify $z_i \rightarrow \{x_{ms,i+1}, x_{ps,i+1}\}$. Go to step 8.

Inclusion of next data point allows increase of function order.

Step 8: Repeat steps 4 through 7 for order $n \rightarrow 1$ and $n \rightarrow n+1$. Go to step 9.

Step 9: Compare 2 different errors. Go to step 10.

$\in_{\min}$ for order 1 with original end points.

$\in_{\min}$ for order 2 with modified end points.

Step 10: Is order 2 better than order 1? If yes, set $n \rightarrow 2$.

Repeat steps 4 through 9 until $\in_{\min,latest} > \in_{\min,previous}$. If no, go to step 11.

Every time order is incremented by 1, number of possible error margins increase.

Step 11: Set $h \rightarrow h+1$. Go to step 12.

Interval 1 has an optimal order 1 and ends at $\{x_{ms,i}, x_{ps,i}\}$.

Step 12: Set $i \rightarrow i+1$, redefine bounds of next interval $z_i \rightarrow \{x_{ms,i}, x_{ps,i}\}$. Go to step 13.

Step 13: Repeat steps 3 through 12 till all intervals or data points are included. Go to step 14.

Step 14: Obtain the Root Mean Square (RMS) of all local minimum errors to generate net scale error.

$\in_{scale} \rightarrow \left\| \in_{\min} \right\|_{RMS}$. Repeat the entire process for form error.

$\varepsilon_{form} \rightarrow \left\| \varepsilon_{\min} \right\|_{RMS}$. Go to step 15.

RMS estimate is used to provide global average of $\in_{\min}$.

Step 15: Estimate system error as $E_{sys} = \in_{RMS} \times \varepsilon_{RMS}$. Go to step 16.

Step 16: Is $E_{sys} \leq \varepsilon_g$? If yes, Print

$n, x_{ps}^{est} = a_1 + b_1 \cos x_{ms} + c_1 \sin x_{ms}$,

$x_m^{est} = a_1^* + b_1^* \cos x_{ms} + c_1^* \sin x_{ms}$ for each interval. End.

If no, print convergence not obtained. End

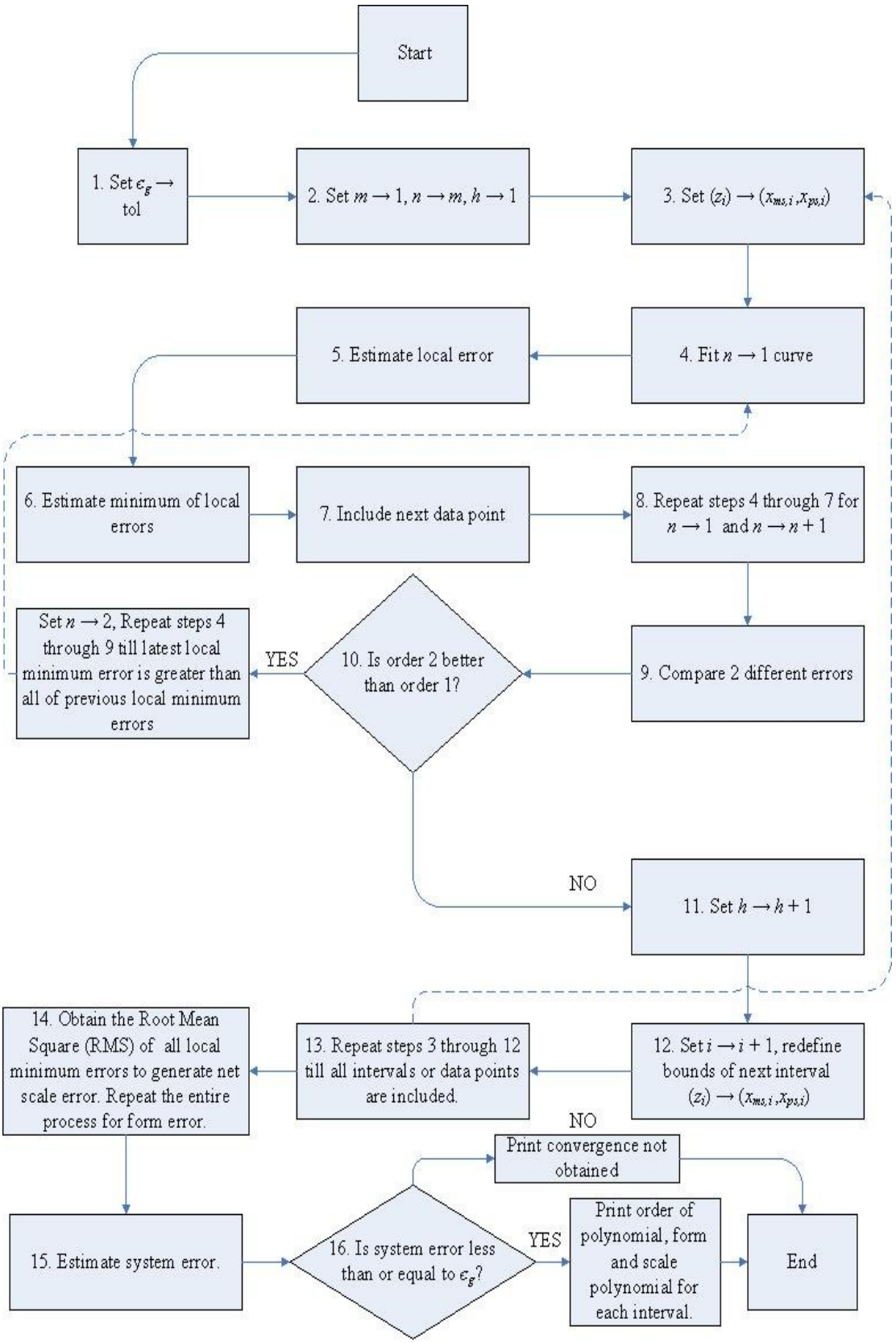

Figure 4. Algorithm for fitting trigonometric functions

ILLUSTRATIVE EXAMPLE – AIRFOIL

Airfoil designs are commonly used to analyze wing behavior in aircrafts, unmanned aerial vehicles (UAV's) and other aerodynamic objects. Airfoils are subjected to intense wind tunnel testing including experimentation for velocity and pressure profiles, drag and lift coefficients and wake regions. To illustrate the applicability of the trigonometric ESM technique in practical designs, we study and predict the values of coefficient of drag in E387 airfoils based on the response of the GEMINI series airfoils focusing on the geometric changes while maintaining the material constant. Notice from the illustration below (see Figure 5) that the GEMINI series airfoils are symmetric across the *x*-axis, a geometric simplification over the asymmetric E387 airfoils. This problem is also a modification of the original ESM formulation as the material properties remain consistent throughout. However, test conditions alter vertically instead of material properties and therefore the analysis is still applicable and pertinent to the ESM ideology albeit in a modified form.

Note also (see Table 1) that the ratio of Reynolds numbers (*Re*) across the *specimen* pair and the *model/product* pair is not consistent – a condition of *distortion*[8]. Development of the *S* and *F* matrices is still possible for such systems due to the potency of the ESM process. [Wood, 2002] studied this system using a linear regression [Edwards, 1976] approach, the results of which do not conform with the required smoothness in solution curve as the analytical relations in linear regression strategies, being point based approximations, do not allow higher order continuity. We show that error can be held in check while enforcing the required continuity conditions using adaptive functions.

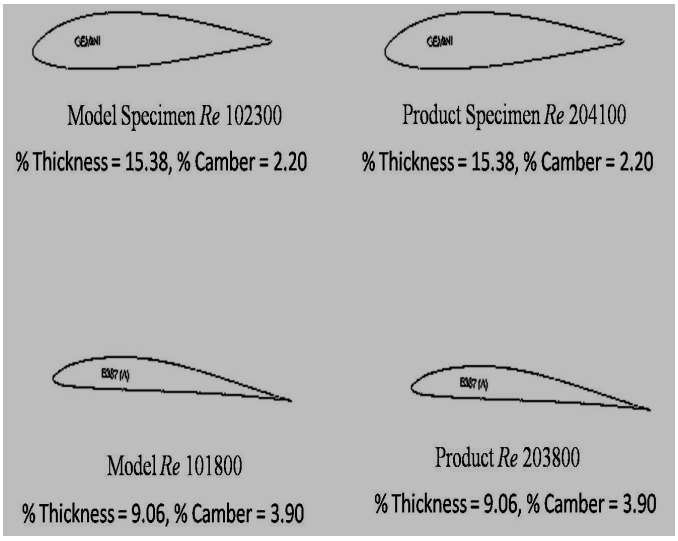

Figure 5. Airfoil system for ESM analysis

[8] Distortion in ESM signifies induced variation or inconsistency in geometry, material properties or test conditions.

Table 1. ESM representation of the airfoil system

Geometry	Test Conditions
Product E387	*Re* 203800
Product Specimen Gemini	*Re* 204100
Model Specimen Gemini	*Re* 102300
Model E387	*Re* 101800

Published experimental data for coefficient of drag (C_d) is used for analysis [Seling et al., 1995] (see Table 2). These values have been measured at discrete points in the four geometries respectively for a specified air velocity and angle of attack. This range of values is of particular interest since the magnitudes are small enough to cause possible singular behavior and issues with matrix evaluations and inversions. However, by inducing adaptivity we ensure that such mathematical obstacles are annulled due to estimation using limited number of points in each interval instead of employing all points together in the global approximation.

Table 2. Measurement data

Measurement	Cd_{ms}	Cd_{ps}	Cd_m	Cd_p
1	0.017600	0.012000	0.027500	0.019400
2	0.016000	0.011750	0.019500	0.014400
3	0.016900	0.011900	0.016600	0.011950
4	0.017200	0.012000	0.016650	0.010650
5	0.019500	0.012350	0.017800	0.010500
6	0.020000	0.012350	0.019800	0.011300
7	0.018600	0.012500	0.021500	0.012300
8	0.018900	0.013150	0.022600	0.013300
9	0.020400	0.014250	0.022950	0.014050
10	0.023800	0.015750	0.022980	0.014600
11	0.025500	0.017800	0.022750	0.015100
12	0.027000	0.020000	0.022700	0.015800
13	0.028500	0.021500	0.023700	0.020200

The next step is to establish the degree of non-linearity to substantiate the use of trigonometric methods which is accomplished by the Pearson's test, the values of coefficients being,

$$r(Cd_{ms}, Cd_{ps}) = 0.9708$$
$$r(Cd_{ms}, Cd_{m}) = 0.4241 \quad (20)$$

The correlation coefficient between the *model* and *model specimen* indicates high non-linearity since the value is much lesser than 1 and thus usage of trigonometric functions is quite relevant. The algorithm is now invoked to estimate interval specific trigonometric functions. The process starts using the first three data points and continues through until the entire set of 13 points is spanned. Both the scale and form trigonometric evaluate to first order functions in the first three intervals spanning the first 7 points. However, the last interval containing the rest of the points is modeled as a third order

variation with 7 degrees of freedom. This is a consequence of mathematical relations and algorithm as the function generating least error is chosen. The resulting transformation matrices are hence developed to be matrices of size 4×7 and their respective values are,

$$S_{Trig.} = \begin{pmatrix} -1.7052E+03 & 1.7052E+03 & 6.5625E-01 & \dots \\ -7.8944E+03 & 7.8944E+03 & 2.7093 & \dots \\ 1.3642E+04 & -1.3642E+04 & -4.7024 & \dots \\ -1.8094E+02 & -6.7648E+02 & 5.2562E+06 & \dots \end{pmatrix}$$

$$\begin{pmatrix} \dots & 0 & 0 & 0 & 0 \\ \dots & 0 & 0 & 0 & 0 \\ \dots & 0 & 0 & 0 & 0 \\ \dots & -5.2206E+03 & 5.2562E+06 & 6.0780E+03 & -5.2562E+06 \end{pmatrix}$$

and

$$F_{Trig.} = \begin{pmatrix} 1.3460E+06 & -1.3460E+06 & -3.8967E+02 & \dots \\ 1.4691E+04 & -1.4691E+04 & -4.2051 & \dots \\ 6.6390E+05 & -6.6390E+05 & -2.2485E+02 & \dots \\ -2.1558E+03 & -3.4517E+03 & 1.8363E+07 & \dots \end{pmatrix}$$

$$\begin{pmatrix} \dots & 0 & 0 & 0 & 0 \\ \dots & 0 & 0 & 0 & 0 \\ \dots & 0 & 0 & 0 & 0 \\ \dots & -1.8020E+04 & 1.8363E+07 & 2.3628E+04 & -1.8363E+07 \end{pmatrix}$$

To compare this trigonometric process to earlier ESM methods, we now introduce a global approach that Cho [1998] developed. This process called the polynomial ESM method is mathematically defined as,

$$x_p = \sum_{i=0}^{n} a_i x_m^i \tag{21}$$

where *n* is the order of the polynomial and the constants a_i's are derived using the relation,

$$x_{ps} = \sum_{i=0}^{n} a_i x_{ms}^i \tag{22}$$

In this case, the system transformation is given by,

$$T = (S \times F) = x_m x_{ms}^{+} \tag{23}$$

where $x_{ms}^{+} = (x_{ms}^{*} x_{ms})^{-1} x_{ms}^{*}$ is the pseudo – inverse of x_{ms} and x_{ms}^{*} is the conjugate transpose of x_{ms} [Albert, 1972]. The prediction equation in this case is written as,

$$x_p = T x_{ps} \tag{24}$$

Unlike the trigonometric approach which is local and adaptive, the polynomial ESM method is global with ambiguity in choice of polynomial order. Since intermediate local errors are not compared to determine the optimal order, the selection of polynomial order is ambivalent and hence the technique is not robust. Further all data points are modeled together increasing complexity and relative concerns with inverting large matrices. For purposes of numerical comparison, we choose a cubic polynomial and contrast the two techniques. The system transformation for the polynomial method is given by,

$$\begin{pmatrix} T_1 \\ T_2 \\ T_3 \\ T_4 \\ T_5 \\ T_6 \\ T_7 \\ T_8 \\ T_9 \\ T_{10} \\ T_{11} \\ T_{12} \\ T_{13} \end{pmatrix}_{Polynomial} = \begin{pmatrix} -0.0592915 & -2.06301 & -0.916047 & -0.540939 & 1.68984 & 1.9484 & \dots \\ -0.0967012 & -2.3542 & -1.06657 & -0.642676 & 1.9029 & 2.20244 & \dots \\ -0.0737667 & -2.17648 & -0.974621 & -0.580488 & 1.7729 & 2.0474 & \dots \\ -0.0592915 & -2.06301 & -0.916047 & -0.540939 & 1.68984 & 1.9484 & \dots \\ -0.0135529 & -1.69614 & -0.727517 & -0.41405 & 1.42084 & 1.62818 & \dots \\ -0.0135529 & -1.69614 & -0.727517 & -0.41405 & 1.42084 & 1.62818 & \dots \\ 0.00380122 & -1.55269 & -0.654234 & -0.364932 & 1.31548 & 1.50296 & \dots \\ 0.0646661 & -1.01878 & -0.384536 & -0.185616 & 0.922227 & 1.03698 & \dots \\ 0.121848 & -0.393993 & -0.0807578 & 0.0108216 & 0.459287 & 0.493732 & \dots \\ 0.130042 & 0.0368277 & 0.101598 & 0.115892 & 0.138198 & 0.128851 & \dots \\ 0.0638797 & 0.160668 & 0.0925774 & 0.0780542 & 0.0520556 & 0.0577229 & \dots \\ -0.0403567 & 0.0778063 & -0.0374765 & -0.0461835 & 0.138408 & 0.197172 & \dots \\ -0.103077 & 0.0391438 & -0.113434 & -0.120022 & 0.193962 & 0.286232 & \dots \end{pmatrix}$$

$$\begin{pmatrix} \dots & 0.995832 & 1.25768 & 2.08482 & 0.835905 & -0.749676 & -1.81718 & -1.66632 \\ \dots & 1.1058 & 1.40579 & 2.3622 & 0.968341 & -0.837368 & -2.05887 & -1.89109 \\ \dots & 1.03877 & 1.31547 & 2.19289 & 0.887345 & -0.784003 & -1.91147 & -1.75396 \\ \dots & 0.995832 & 1.25768 & 2.08482 & 0.835905 & -0.749676 & -1.81718 & -1.66632 \\ \dots & 0.856117 & 1.07009 & 1.73555 & 0.67131 & -0.637116 & -1.51129 & -1.38243 \\ \dots & 0.856117 & 1.07009 & 1.73555 & 0.67131 & -0.637116 & -1.51129 & -1.38243 \\ \dots & 0.801064 & 0.99639 & 1.5991 & 0.607818 & -0.592354 & -1.39122 & -1.27118 \\ \dots & 0.593254 & 0.719688 & 1.09232 & 0.377586 & -0.420771 & -0.941469 & -0.855551 \\ \dots & 0.33987 & 0.387894 & 0.505202 & 0.131264 & -0.203212 & -0.407426 & -0.36453 \\ \dots & 0.144645 & 0.144232 & 0.119196 & 0.0132931 & -0.0220479 & -0.0312501 & -0.0194775 \\ \dots & 0.0488312 & 0.0485838 & 0.0632851 & 0.0946037 & 0.0837566 & 0.071943 & 0.0840385 \\ \dots & 0.0347972 & 0.0675801 & 0.240636 & 0.292721 & 0.108236 & -0.04117 & 0.00782891 \\ \dots & 0.0272564 & 0.0807206 & 0.353565 & 0.412117 & 0.1122 & -0.125215 & -0.0434483 \end{pmatrix}$$

Notice the complexity and heavily populated matrix of size 13×13 developed to model the data. This is due to the fact that all 13 data points are included in the analysis together instead of working with smaller and manageable intervals. Thus global methods tend to develop fairly large matrices resulting in significant cost and time during matrix inversion. The global polynomial approach also does not yield greater accuracy which we compare using equation 10, to trigonometrically predict the values summarized below (see Table 3) along with the global approximation cubic polynomial[9] values, predicted using equation 24.

[9] A cubic polynomial is also constructed that is global to contrast the two schemes *i.e.*, local adaptive trigonometric polynomial *vs*. global non-adaptive cubic polynomial.

Table 3. Prediction and error values

Measurement	Cdp - Trigonometric	Error	Cdp - Polynomial (3rd Order)	Error
1	0.018530	4.48%	0.012120	37.53%
2	0.012198	15.29%	0.0115213	19.99%
3	0.011820	1.09%	0.0118834	0.56%
4	0.011807	10.86%	0.012120	13.80%
5	0.012479	18.84%	0.0129184	23.03%
6	0.012343	9.23%	0.0129184	14.32%
7	0.013649	10.97%	0.0132468	7.70%
8	0.015326	15.23%	0.0145768	9.60%
9	0.015576	10.86%	0.0165039	17.47%
10	0.015598	6.84%	0.0185445	27.02%
11	0.015432	2.20%	0.0204209	35.24%
12	0.015396	2.56%	0.0215535	36.41%
13	0.016149	20.05%	0.0219757	8.79%
RMS Error		11.58%		22.47%

Notice that the adaptive trigonometric ESM process produces a more accurate solution when compared to the global cubic polynomial. Another interesting outcome is that the trend or variation of the solution curve is well-defined and conforming to the actual variation (see Figure 6) as against the cubic polynomial curve whose trend is significantly different from the actual solution. Thus proper evolution of solution curve is guaranteed in the trigonometric process due to adaptivity and discretization, and smoothness is ensured by forcing first order continuity – both mathematical features contributing immensely to the development of final solution in terms of accuracy and trend respectively.

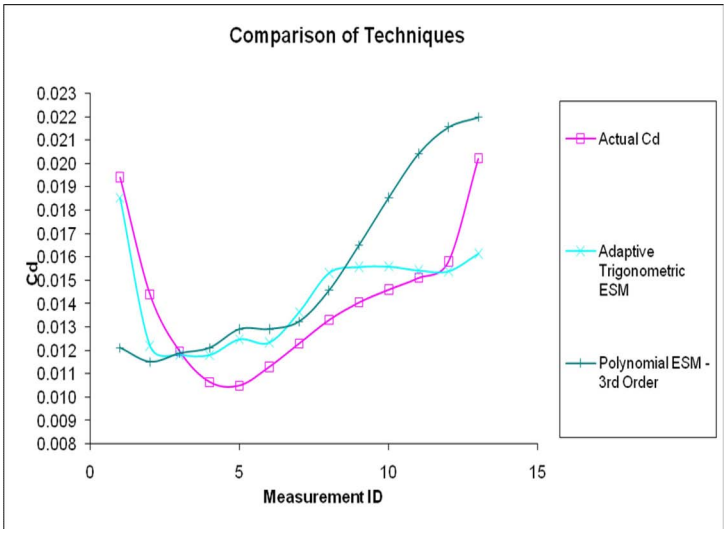

Figure 6. Comparison of techniques

CONCLUSIONS

Based on the use of modern numerical tools, we have examined in this paper, use of empirical similitude method in its modified form. Using correlation tests, we have motivated the use of advanced numerical patterns such as trigonometric function approximation and elaborated on the need to ensure smooth and continuous solutions through the use of adaptive considerations. Extending ESM and numerical analysis, we have developed and shown an error minimizing approach and applied it to an airfoil system whose values of coefficient of drag have been predicted. Considerable improvement has been attained (as indicated by the accuracy margins) compared to earlier ESM techniques. Other adaptive models including splines and regression techniques are also being pursued.

References

[1] Albert, A., 1972, *Regression and the Moore – Penrose Pseudoinverse*, Academic Press.

[2] Baker, W. E., Westine, P. S., Dodge, F. T., 1991, *Similarity Methods in Engineering Dynamics: Theory And Practice of Scale Modeling*, Elsevier.

[3] Broeren, A. P., Giguere, P., Guglielmo, J. J., Selig, M. S., 1995, *Summary of Low-Speed Airfoil Data*, Vol. 1, SoarTech Publications, Virginia Beach, Virginia.

[4] Binder, R. C., 1973, *Fluid Mechanics*, 5th Edition, Prentice-Hall, Englewood Cliffs, N.J.

[5] Cho, U., Wood, K., 1997, *Empirical Similitude Method for the Functional Test with Rapid Prototypes*, Proceedings of the Solid Freeform Fabrication Symposium, Austin TX, September, 1997, pp. 559-567.

[6] Cho, U., Wood, K. L., Crawford, R. H., 1998b, *Novel empirical similarity method for the reliable product test with rapid prototypes*, Proceedings of DETC, Atlanta, GA, September 13-16, 1998.

[7] Cho, U., Wood, K. L., Crawford, R. H., 1998, *Online Functional Testing with Rapid Prototypes: a Novel Empirical Similarity Method*, Rapid Prototyping Journal, 4, No. 3, pp. 128-138.

[8] Cho, U., 1999, *Novel Empirical Similarity Method for Rapid Product Testing and Development*, Doctoral dissertation, The University of Texas at Austin.

[9] David, F. W., Nolle, H., 1982, *Experimental Modelling In Engineering*, ButterWorths.

[10] Dornfeld, W. H., 1995, *Direct Dynamic Testing of Scaled Stereolithographic Models*, Sound and Vibration, August, 12-17.

[11] Dutson, A. J, 2002, *Functional Prototyping Through Advanced Similitude Techniques*, Doctoral dissertation, The University of Texas at Austin.

[12] Edwards, A. L., 1976, *An Introduction to Linear Regression and Correlation*, W. H. Freeman, San Francisco, CA.

[13] Kendell, A. A., 1988, *An Introduction to Numerical Analysis*, 2nd Edition, Section 8.9, John Wiley and Sons.

[14] Langhaar, H. L., 1951, *Dimensional Analysis and Theory of Models*, John Wiley & Sons, New York.

[15] Linz, P., 1979, *Theoretical Numerical Analysis: An Introduction to Advanced Techniques*, Wiley, New York.

[16] Schnittger, J. R., 1988, *Dimensional Analysis in Design*, Journal of Vibration, Acoustics, Stress and Reliability in Design, Vol. 110, January-February, 401-406.

[17] Spiegel, M. R., 1992, *Theory and Problems of Probability and Statistics*, 2nd Edition, McGraw-Hill, New York.

[18] Wood, J. J., 2002, *Design Methodology using Empirical and Virtual Analysis with Application to Compliant Systems*, Doctoral dissertation, Colorado State University.